МИНЕРАЛЫ И МИНЕРАЛЬНЫЕ ПАРАГЕНЕЗИСЫ

NEW DATA ON Bi-, Pb-BEARING AND Mn-RICH GEM TOURMALINE FROM THE MALKHAN PEGMATITE DISTRICT (TRANSBAIKALIA)

© 2022 г. O. S. Vereshchagin[a], *, A. V. Kasatkin[b], and R. Škoda[c]

[a] *Mineralogical Department, Institute of Earth Sciences, Saint Petersburg State University, University Emb., 7/9, Saint Petersburg, 199034 Russia*

[b] *Fersman Mineralogical Museum RAS, Leninsky Prospekt, 18-2, Moscow, 119071 Russia*

[c] *Department of Geological Sciences, Faculty of Science, Masaryk University, Kotlářská, 2, Brno, 611 37, Czech Republic*

**e-mail: o.vereshchagin@spbu.ru*

Received September 23, 2022; Revised October 4, 2022; Accepted October 12, 2022

Lead or/and Bi-bearing tourmalines are rare in nature while Mn-bearing ones are quite common. Here, we present new data on Bi- (up to ~2 wt % Bi_2O_3), Pb-bearing (up to ~2 wt % PbO) and Mn-rich (up to ~5 wt % MnO) tourmalines from the Irkutianka vein and Mn-rich tourmalines (up to ~6.5 wt % MnO) from the Novaya vein, both occurring at the Malkhan pegmatite district. Four gem-quality tourmalines (sm21-1, sm21-2, sm21-3, and sm21-4) of different color (yellow, colorless and red) and morphology (elongated and flattened) from the Irkutianka vein were studied by optical and scanning electron microscopy (SEM) and energy dispersive analysis (EDS). Two samples (1015f and 1377f) of gemmy yellow tourmaline from the Novaya vein were additionally examined using WDS and LA-ICP-MS. All the studied tourmalines from the Irkutianka vein belong to fluor-elbaite – fluor-liddicoatite series and show the Na/Ca and Li/Mn/Fe zonation. The tourmalines from the Novaya vein, instead, do not show any zonation and belong to Mn-rich (up to 0.88 *apfu* Mn) fluor-elbaite. The complex chemical zonation observed for transitional metal contents resulted in the appearance of color (or a lack of it). Colorless tourmaline sm21-4 has constant Bi impurity, whose amount decreases from the rim to the core (from 0.09 to 0.01 *apfu*) of the crystal in question. This tourmaline is among the Bi-richest species discovered so far. Lead was detected in rose-to-colorless tourmaline sm21-3 and colorless one sm21-4. Only the inner parts of the tourmaline sm21-3 contain lead (<0.2 wt % PbO), while the Pb-richest domains (up to 30 mμ in size; Pb up to 0.09 *apfu*) were discovered in the core of the tourmaline sm21-4. We suppose that both Pb^{2+} and Bi^{3+} occupy the nine-coordinated *X*-site in the tourmaline crystal structure.

Keywords: tourmaline, gem, Pb, Bi, Mn, Malkhan

DOI: 10.31857/S0869605522060077

1. INTRODUCTION

Tourmaline is equally well known to materials scientists, geologists and gemologists for its unique combination of properties. It is a promising material with piezoelectric (e.g., Li et al., 2012), pyroelectric (e.g., Chernyshova et al., 2021), and ultraviolet optical nonlinear properties (Xia, Kang, 2022). It is stable in a wide range of temperatures and pressures (e.g., Van Hinsberg et al., 2011), is one of the most important carriers of boron (e.g., Sunde et al., 2020), and reflects its formation conditions in the chemical composition (e.g., Baksheev et al., 2012). The colors diversity of tourmaline and its geminess make it suitable for use in jewelry (e.g., Pezzotta, Laurs, 2011).

Tourmaline supergroup minerals have the generalized chemical formula $^{[9]}X^{[6]}Y_3{}^{[6]}Z_6$ ($^{[4]}T_6O_{18}$)($^{[3]}BO_3)_3V_3W$ (Henry et al., 2011). According to Henry et al. (2011), tourmaline can be classified into primary groups based on the dominant occupancy of the *X*-site. Twenty-one members of the tourmaline supergroup contain Na as the dominant cation at the *X*-site, seven – Ca, six – □ (vacancy) and only one – K. However, recent advances in tourmaline synthesis coupled with single crystal *X*-ray data (SCXRD) confirmed that Ag^+ (London et al., 2006), Li^+ (Kutzschbach et al., 2014), $NH_4{}^+$ (Wunder et al., 2015), Ln^{3+} (Ln^{3+}=La, Eu, Nd, Yb) (Vereshchagin et al., 2021) and Pb^{2+} (Vereshchagin et al., 2020) could also be present at the *X*-site in sufficient amounts.

Interestingly, the published data showed that Pb-rich tourmalines could be found in nature. The first data on Pb-bearing tourmalines were described by Lebedev (1937) who investigated Fe-rich tourmalines with 1.1% Pb from Malyi Khingan, Russia. Since then, Pb-rich tourmalines have been reported in Momeik, Myanmar (up to 1640 ppm Pb; Ertl et al., 2007), Eastern Alps, Austria (up to 0.5 wt % PbO_2; Ertl et al., 2019), Madagascar (up to 0.5 wt % PbO; Lussier, Hawthorne, 2011), Malkhan pegmatite field, Russia (up to 0.5 wt % PbO; Peretyazhko et al., 1989), Alto Ligonha area, Mozambique (up to 15.4 wt % PbO; Sokolov, Martin, 2009) and the Minh Tien pegmatite, Vietnam (up to 17.5 wt % PbO; Sokolov, Martin, 2009; Kubernátová, Cempírek, 2019). Lead-rich tourmaline (with 17.5 wt % of PbO) falls into the Pb dominant field. However, the Pb-richest tourmalines are very narrow zones complicating extraction and no Pb-dominant tourmaline has been recognized as a mineral species to date.

The examples of Bi-bearing tourmaline are relatively uncommon and no proof of the Bi incorporation into the tourmaline crystal structure has been gained. The first data on Bi-bearing tourmalines were obtained by Staatz et al. (1955) who noted trace amounts of Bi in Li-rich Brown Derby pegmatite, USA. Later Bi-bearing tourmalines were reported in Lundazi, Zambia (up to 0.49 wt % Bi_2O_3; Johnson et al., 1997), Malkhan pegmatite field, Russia (up to 0.5 wt % Bi_2O_3; Peretyazhko et al., 1989), São José da Batalha, Brazil (up to 0.83 wt % Bi_2O_3; Fritsch et al., 1990; Henn et al., 1990; Rossman et al., 1991), Edeko, Nigeria (up to 10540 ppm Bi (~1.18 wt % Bi_2O_3); Abduriyim et al., 2006) and Alto Ligonha, Mozambique (up to 19480 ppm Bi (~2.17 wt % Bi_2O_3); Abduriyim et al., 2006). It is worth noting that Ertl et al. (2007) and Ertl, Bačík (2020) suggested that Bi could be incorporated at the *X*-site of the tourmaline crystal structure. Though the Bi content of the sample studied by Ertl et al. (2007) was only 143 ppm and Na + Ca + Pb + vacancies were simultaneously present at the *X*-site, which precludes an unambiguous interpretation of the SCXRD.

In the contrary to the above, Mn-bearing tourmalines are relatively common in nature and have been subject of many publications (see, e.g., Burns et al., 1994; Bosi et al., 2012, 2015; Ertl et al., 2003, 2012, etc.). Moreover, four tourmaline supergroup members are known to contain Mn as species-defining element, namely tsilaisite (Bosi et al., 2012), fluor-tsilaisite (Bosi et al., 2015), celleriite (Bosi et al., 2022a), and princivalleite (Bosi et al., 2022b).

The aim of this study is to obtain the data on the chemical composition of gem Pb-, Bi-bearing and Mn-rich tourmalines from the Irkutianka and Mn-rich tourmalines from the Novaya pegmatite veins, Malkhan pegmatite district, Russia, and discuss possible mechanisms of Pb and Bi cations' incorporation into the tourmaline crystal structure.

2. GEOLOGICAL SETTINGS AND EXPERIMENTAL METHODS

The Malkhan pegmatite district is among the most famous tourmaline deposits, which represents the largest source of gem-grade and specimen-quality tourmaline in Russia. The deposit is located in the Krasny Chikoy area of the Zabaikalskiy Krai, Transbaikalia, Russia. The geology, mineralogy, and geochemistry of the pegmatite field are described in detail by Zagorsky and Peretyazhko (1992), Zagorsky et al. (1999), Zagorsky (2010, 2015). The Malkhan pegmatite field is confined to the Bolsherechensky and Oreshny massifs of Lower Cretaceous biotite granites and two-mica leucogranites, whereas pegmatites themselves occur as slab-like vein bodies up to 350 m long and up to 7–10 m thick among the rocks of the Malkhan complex

(Zagorsky, 2015). There are more than 15 tourmaline-bearing veins in the Malkhan pegmatite district, the most important among them are Danburitovaya, Geologicheskaya, Irkutianka, Karkadilovaya, Mokhovaya, Novaya, Oktyabrskaya, Oreshnaya, Skakunya, Solnechnaya, Sosedka, Svetlaya, Tabornaya, Zapadnaya-1 and Zimoveynaya. It is pertinent to note that one of the characteristic features of the several pegmatite bodies of the Malkhan field is their enrichment in bismuth (e.g., Peretyazhko et al., 1992). To date, nine minerals with species-defining Bi were identified (Peretyazhko et al., 1992; Badanina et al., 2008; Kasatkin et al., 2021; our data): native bismuth, bismuthinite, bismutite, bismite, bismutocolumbite (a new mineral species discovered in the Danburitovaya pegmatite vein, Peretyazhko et al., 1992), bismutotantalite, cannonite, oxybismutomicrolite (a new mineral species discovered in the Solnechnaya pegmatite vein, Kasatkin et al., 2021) and wittichenite. It is also interesting to note, that no minerals with species defined Pb were found in the Malkhan pegmatite district.

The tourmalines used for this study were collected during field works at the Irkutianka pegmatite vein in summer 2021 and at the Novaya vein – in 2016 (sample 1015f) and 2021 (sample 1337f). Four tourmaline crystals of different color and morphology from the Irkutianka vein (Figs. 1, 2) and two matrix samples from Novaya vein (Fig. 3) were selected for further studies. Their appearance was studied using a Leica DM 2500P polarizing light microscope. Next the crystals were epoxy mounted, cut perpendicular to the elongation, polished and carbon-coated. The chemical composition of the crystals from the Irkutianka pegmatite vein was analyzed by means of a Hitachi S-3400N SEM equipped with an AzTec Energy X-Max 20 EDS using natural and synthetic compounds as analytical standards. The chemical composition of the crystals from Novaya pegmatite vein was examined with a Cameca SX-100 electron microprobe (WDS mode, 15 kV, 10 nA, 8 μm beam diameter). Peak counting times (CT) were 20 s for major elements and 60 s for minor elements; CT for each background was one-half of the peak time. The fluorine *K*a line interferes with the Fe and Mn*L*a lines, requiring a correction for the measured F values. Analyzed elements, analytical *X*-ray lines and standards were as follows: F*K*α – topaz; Na*K*α – albite; Al*K*α and K*K*α – sanidine; Si*K*α – almandine; Ca*K*α – fluorapatite; Ti*K*α – titanite; Mn*K*α – spessartine; Zn*K*α – gahnite. Other elements heavier than F were sought but their contents were below detection limit. The raw intensities were converted to concentrations using *X-PHI* (Merlet 1994) matrix-correction software.

The lithium content in tourmalines from the Irkutianka vein was calculated using the equation obtained by Pesquera (2016). Concentrations of Li in tourmalines from the Novaya vein were investigated by LA-ICP-MS using an Agilent 7500ce quadrupole ICP-MS with an attached UP 213 laser ablation system. The samples were placed into a SuperCell having a volume of 33 cm^3 and ablated using a commercial Q-switched Nd:YAG laser operated at a wavelength of 213 nm (pulse duration 4.2 ns). Ablated material was transported from the sample chamber using helium carrier gas (1 L/min) and mixed with argon (0.6 L/min) prior to the torch. Optimization of LA-ICP-MS parameters (gas flow rates, sampling depth, voltage of ion optics) was performed using glass reference material NIST SRM 610 and 612 to maximize the S/N ratio. Potential polyatomic interferences were minimized by a collision reaction cell in He mode (2.5 mL/min).

The empirical formulae of all tourmalines were calculated on the basis of 15 ($T + Y + Z$) atoms per formula unit (*apfu*) considering that: (1) vacancies may occur at the *X*-site, (2) lead and bismuth occur at the *X*-site as divalent and trivalent cations, respectively, (3) there is no excess of boron (B = 3 *apfu*). The H_2O content was calculated on the basis of OH + F = 4 *apfu*.

3. RESULTS AND DISCUSSION

The Irkutianka tourmalines studied macroscopically have various colors and zonations. Sample sm21-1 is a prismatic tourmaline crystal (2.5 × 0.8 cm) of yellowish color, covered by colorless platy mica (Fig. 1*a*). The tourmaline crystal has a rose to colorless core (Fig. 1*b*) and a yellowish rim with 2 distinct zones (Figs. 1*c*, 1*d*). Samples sm21-2 and sm21-3 are also represented by prismatic tourmaline crystals (2.4 × 0.5 and 2 × 0.8 cm, respectively) of bright yellow and rose colors, respectively (Figs. 1*e*, 2*a*). Sample sm21-2 has a yellow core and a colorless rim (Fig. 1*f*) with zonation (Figs. 1*g*, 1*h*). Sample sm21-3 has a colorless bottom and a rose

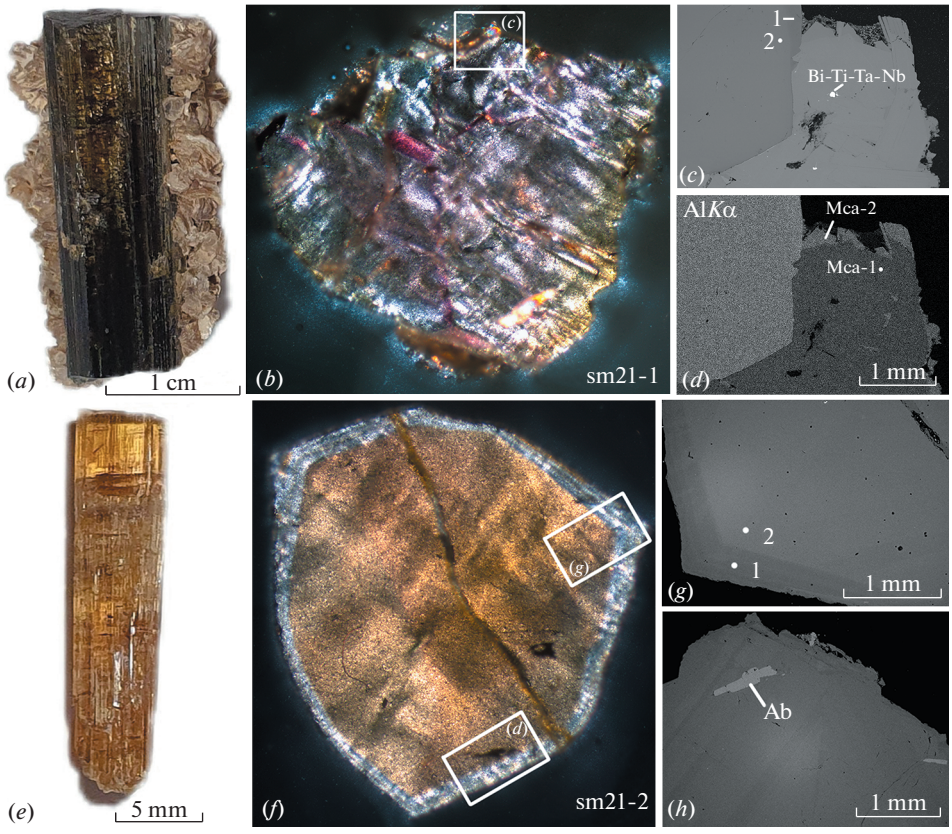

Fig. 1. Zonation in yellowish tourmalines from the Irkutianka vein: (*a*–*d*) sample sm21-1, (*e*–*h*) sample sm21-2. (*a*) columnar tourmaline crystal with mica, (*b*) yellow rim on an orange to rose core of a tourmaline cut, (*c*) mica overgrowth on zoned tourmaline, (*d*) Al distribution map (Al*K*α), (*e*) columnar tourmaline crystal, (*f*) colorless rim on a yellow core of a tourmaline cut, (*g*) thin zoning in the rim, (*g*) albite (Ab) inclusion inside tourmaline. Note: numbers are those in Table 1, Ab, albite, Mca, mica, Bi-Ti-Ta-Nb, *X*-ray amorphous Bi-rich phase.

Рис. 1. Зональность в желтых кристаллах турмалина жилы Иркутянка: *a*–*d* – обр. sm2-1, *e*–*h* – обр. sm21-2. (*a*) столбчатый кристалл турмалина со слюдой, (*b*) желтая кайма на оранжево-розовой центральной части кристалла турмалина, (*c*) нарост слюды на зональном турмалине, (*d*) карта распределения Al (Al*K*α), (*e*) столбчатый кристалл турмалина, (*e*) – бесцветная кайма на желтой центральной части кристалла турмалина, (*g*) – тонкая зональность в кайме, (*h*) – включение альбита внутри турмалина. Примечание: номера анализов соответствуют номерам в табл. 1. Ab – альбит, Mca – слюда, Bi-Ti-Ta-Nb – рентгеноаморфная фаза.

top, which was cut and analyzed. The tourmaline cut of sample sm21-3 has complex zonation and sectorial growing with at least 4 different blocks (Figs. 2*b*–2*c*). Sample sm21-4 is represented by a single tourmaline crystal (3.5 × 1.5 cm), which has a flattened hexagon cut (Fig. 2*e*) instead of a Reuleaux triangle typical for tourmalines. This tourmaline has a rose homogeneous core and a colorless to red rim (Fig. 2, *f*) with complex zonation (Figs. 2, *g*, 2*h*).

Two out of four samples from the Irkutianka vein contain mineral inclusions/associated minerals besides tourmaline. SEM EDX data showed that white mica in sample 21-1 overgrows tourmaline and has zonation (Mca1 and Mca2; Fig. 1, *d*). The earliest generation of mica (Mca1) started to grow when the tourmaline core was formed. It has quite a simple composition (SiO_2 ~ 49.4, Al_2O_3 ~ 30.7, K_2O ~ 11.9, F ~ 1.9 wt %). The outer zone of mica (Mca2) has a much more complex composition (SiO_2 ~ 54.1, Al_2O_3 ~ 21.0, K_2O ~ 10.9, TiO_2 ~ 0.3,

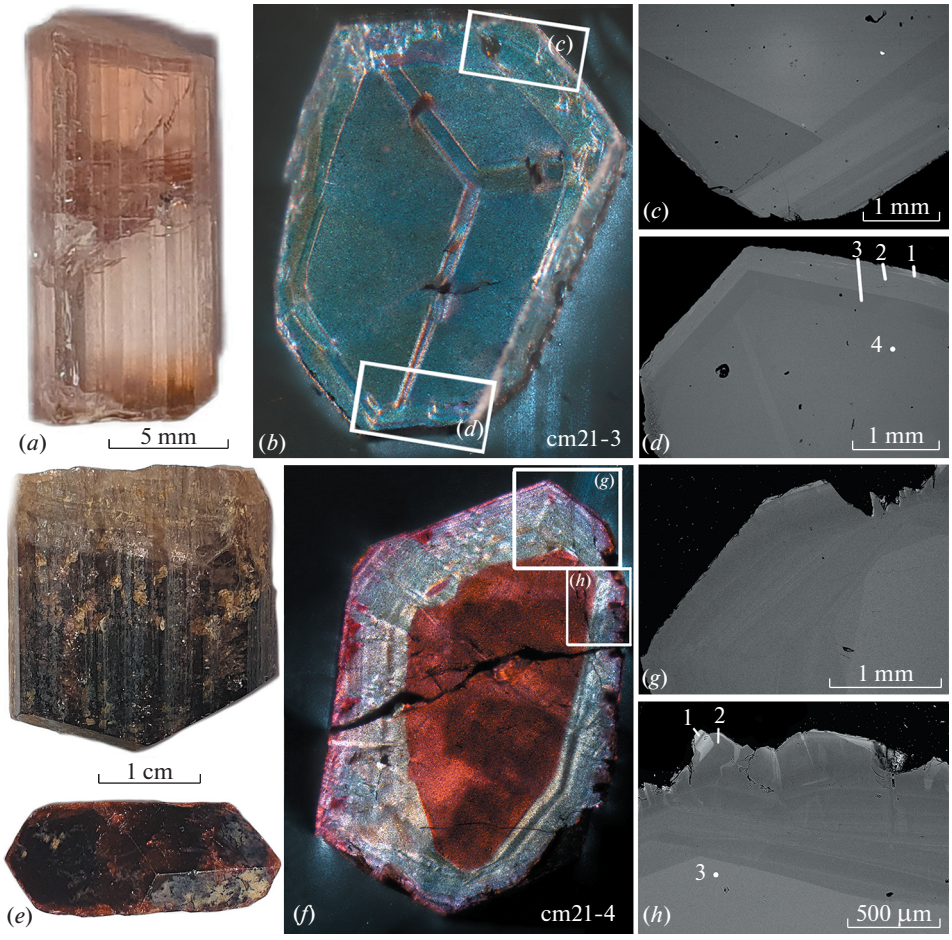

Fig. 2. Zonation in rose tourmalines from the Irkutianka vein: (*a*–*d*) sample sm21-3, (*e*–*h*) sample sm21-4. (*a*) columnar crystal with a rose top and a colorless bottom, (*b*) complex sectorial zoning of a tourmaline cut, (*c*) complex zonation of the rim part of a tourmaline crystal, (*d*) Bi-rich outer zone of the crystal, (*e*) flattened tourmaline crystal, (*f*) complex rose to colorless rim on the red core of a tourmaline cut, (*g*) complex zonation of the rim of a crystal, (*h*) Pb-rich outer zone of a crystal. Note: numbers are those in Table 1.

Рис. 2. Зональность в розовых кристаллах турмалина жилы Иркутянка: *a*–*d* – обр. sm21-3, *e*–*h* – обр. sm21-4. (*a*) столбчатый кристалл с розовой вершиной и бесцветным основанием, (*b*) сложная секториальность и зональность в окраске турмалина, (*c*) сложная зональность краевой части кристалла турмалина, (*d*) богатая висмутом внешняя зона кристалла, (*e*) уплощенный кристалл турмалина, (*f*) розово-бесцветная кайма, обрастающая красную центральную часть кристалла турмалина, (*g*) сложная зональность каймы кристалла, (*h*) богатая свинцом внешняя зона кристалла. Примечание: номера анализов соответствуют номерам в табл. 1.

MnO ~ 0.6, Na_2O ~ 0.2, Cs_2O ~ 0.8, F ~10.3 wt %) and contains a significantly greater amount of F (almost 5 times higher). Both generations of mica could be considered as members of muscovite–trilithionite–polylithionite series, since no direct information on Li and B is available. An interesting unidentified Bi-rich *X*-ray amorphous phase (up to 50 μm) was found inside the first generation (Mca1) of mica. This phase contains (wt %): Bi_2O_3 ~ 37.7, Ta_2O_5 ~ 14.4, Nb_2O_5 ~ 13.5, TiO_2 ~ 12.9, Sb_2O_3 ~ 4.6, SnO_2 ~ 3.1, UO_2 ~ 3.1, CaO ~ 1.2, MnO ~ 1.0, ThO_2 ~ 0.6. On the basis of its isometric shape and chemical composition we can

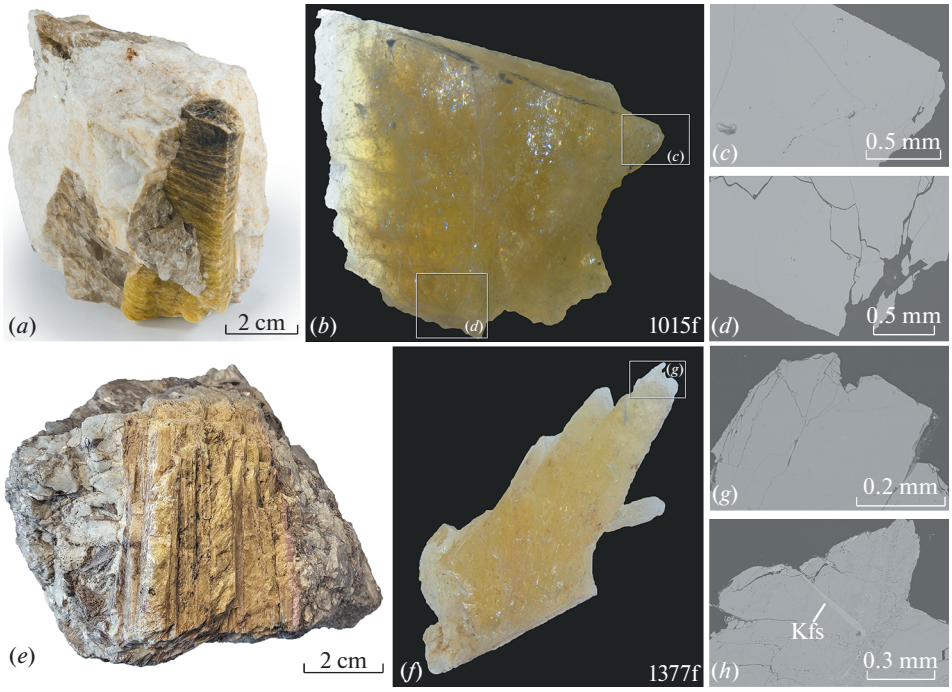

Fig. 3. Yellow Mn-rich fluor-elbaites from the Novaya vein: (*a–d*) sample 1015f, (*e–h*) sample 1377f. (*a*, *e*) general views, (*b*, *f*) polished section cuts, (*c, d, g, h*) SEM (BSE) photos. (*h*) potassic feldspar (Kfs) inclusion inside tourmaline.

Рис. 3. Кристаллы желтого фтор-эльбаита, обогащенные марганцем, из жилы Новая: *a–d* – обр. 1015f, *e–h* – обр. 1377f. *a, e* – общий вид, (*b, f*) – полированная пластина, (*c, d, g, h*) – изображения в отраженных электронах, (*h*) включение калиевого полевого шпата (Kfs) внутри турмалина.

suggest that it is a microlite group mineral, whose crystallinity was lost due to the high content of U and Th. Besides, an elongated albite inclusion was found inside the tourmaline crystal in sample sm21-2 (Fig. 1, *h*).

Three out of four tourmalines from the Irkutianka vein (samples sm21-1, sm21-2, sm21-4) are represented by Na-dominant species (Na > Ca > □), whereas one tourmaline (sm21-3) mainly has a Ca-dominant composition (Table 1). All the tourmalines in question contain Li (0.73–1.38 *apfu*) and Al (7.22–7.72 *apfu*) in octahedral sites. The aluminum content should be present in both YO_6 and ZO_6 octahedral sites as it is significantly greater than 6 *apfu* and all tourmalines are Li-rich. Other octahedral cations (Mn, Fe, Ti) comprise less than 1 *apfu*. The tourmalines do not show any lack of Si (5.90–6.02 *apfu*) and are represented by F-dominant species (0.61–0.92 *apfu*). According to our chemical data, they could be considered as members of fluor-elbaite, $Na(Li_{1.5}Al_{1.5})Al_6(Si_6O_{18})(BO_3)_3(OH)_3F$, (sm21-4, sm21-2, sm21-2 and sm21-3, analysis No. 3) – fluor-liddicoatite, $Ca(Li_2Al)Al_6(Si_6O_{18})(BO_3)_3(OH)_3F$, (sm21-3, analyses No. 1, 2, 4) series.

The tourmalines from the Novaya vein are yellow to pale yellow in very thin fragments (Figs. 3, *b*, *f*) and, differently from the Irkutianka tourmalines, show no sign of zonation (Figs. 3 *c*, *d*, *g*, *h*). Sample 1015f contains a large 8 × 3 cm cluster of yellow prismatic crystals of tourmaline in potassic feldspar and quartz. Sample 1377f represents a big (5 × 4 cm) partial yellow crystal embedded in pegmatitic rock (albite, potassic feldspar, muscovite, fluorluanshiweiite). Tourmaline crystal from sample 1015f is free of inclusions while one extracted from the sample 1377f contains rare and very small inclusions of pyrophanite, nioboixiolite-(Mn), and potassic feldspar (Fig. 3, *h*). Tourmaline analyses demonstrate very narrow range of all detected elements (Table 1) and attribution of both

studied specimens to one tourmaline member – fluor-elbaite. The remarkable feature of these tourmalines is their enrichment in Mn – up to 6.53 wt %, or 0.88 *apfu* (Table 1), however, it does not affect their assignment as fluor-elbaite. Indeed, they are Na-dominant at the *X*-site and F-dominant at *W*-site. Thus, with regard to the *Y*-site, the formula electroneutrality requires that the total charge at *Y* is +6 in the end-member formula: $Na(Y_3)^{\Sigma 6+}Al_6(Si_6O_{18})(BO_3)_3(OH)_3F$. This can be achieved in various atomic arrangements of which elbaitic one [$^{Y}(Li_{1.5}Al_{1.5})$] is dominant.

Such Mn-rich fluor-elbaites are not unique. Burns et al. (1994) reported on crystal chemistry of yellow tourmalines from Nepal (up to 5.97 wt % MnO) and Zambia (up to 6.23 wt % MnO). Similar compositions were reported from Malkhan pegmatite field (up to 4.50 wt % MnO), pegmatites of Central (up to 5.45 wt % MnO) and South-Eastern (up to 5.50 wt % MnO) Pamir Mts. in Tajikistan, and Little Three Mine in California, USA (6.05 wt % MnO) (Zagorsky et al., 1999).

The color of tourmalines reflects the content of transition metals inside them. The yellow color of tourmalines from the Novaya vein is typical for Mn^{2+}-rich tourmalines (Burns et al., 1994; Rossman, Mattson, 1986; Simmons et al., 2011). The core of sample sm21-1 from the Irkutianka has higher Mn and Fe contents compared to the colorless core (0.66 and 0.26 *apfu vs.* 0.34 and 0.11 *apfu*, respectively; Table 1). An inverse color change (a yellow core and a colorless rim) coupled with the increased contents of Mn and Fe was also observed in sample sm21-1. Sample sm21-3 does not contain any Fe or Mn, which is reflected in the absence of color. Interestingly, a high Mn content (up to 0.38 *apfu*) was also revealed in the red core and the outer rim of sample sm21-4 (Table 1). Previously Ertl et al. (2012) showed that the red color of Mn-enriched tourmalines could be caused by Mn^{3+}. Thus we can conclude that this flattened tourmaline was probably formed in oxidizing conditions, which differed significantly from those of samples sm21-1 and sm21-2.

Differently from Mn, both lead and bismuth are not chromophore elements (e.g., Whitmire, 2004; Swadźba-Kwaśny, 2015). Since they are heavy elements, their presence should increase both the specific gravity and refractive index (e.g., Bloss et al., 1983) but neither of these properties appears to have been measured in Pb-/Bi-rich natural tourmalines yet. However, their presence could help to track the origin of the tourmalines, as the identification of gem-tourmalines is rather complicated.

The bismuth content of the samples under consideration could reach 2.08 wt % Bi_2O_3 (Table 1), which is much higher than the previously reported value for the tourmalines from the Zapadnaya-1 pegmatite vein (up to 0.49 wt % Bi_2O_3; Peretyazhko et al., 1989) and among the highest values discovered in tourmalines so far. Colorless tourmaline sm21-4 has a constant Bi impurity, whose amount decreases from the rim to the core (from 0.09 to 0.01 *apfu*). The calcium and sodium contents in different tourmaline zones/sectors do not correlate with each other and/or Bi. Moreover, we did not observe any significant correlation between the Bi content and any other detected element, which could be due to the absence of the direct data on Li and B. The bismuth content of sample sm21-3 is relatively small (up to 0.32 wt % Bi_2O_3; Table 1), but it was also detected in the outer zone of the crystal. It is worth noting that the tourmaline in sample sm21-1 is Bi-free, though it was found in association with a Bi-rich "microlite". This could reflect different crystallization medium conditions during their formation as Bi-free tourmalines contain Mn^{2+}, while Bi-bearing tourmalines contain Mn^{3+}.

The lead content in the tourmalines under investigation could reach 2.09 wt % PbO (Table 1), which is also much higher than the one that was previously reported in the Zapadnaya-1 pegmatite vein (up to 0.54 wt % Bi_2O_3; Peretyazhko et al., 1989). However, the Pb content in Malkhan's tourmalines is much smaller than that of the tourmalines discovered in amazonite granites of Alto Ligonha or Minh Tien (up to 17.5 wt % PbO (~0.9 *apfu* Pb); Sokolov, Martin, 2009). Lead was detected in samples sm21-3 and sm21-4 (Table 1). Only the inner parts of the tourmaline sm21-3 contain lead (<0.2 wt % PbO), while the Pb-richest zones were discovered in the core of the tourmaline sm21-4. The zones are small (up to 30 μm in size) and were formed in a process of cracking and dissolution of the main tourmaline "body" (Fig. 2*h*).

Both Bi and Pb occur in nature as Bi^{3+} and Pb^{2+} minerals and their aqueous chemistry precludes penta- and tetravalent oxidation state (for Bi and Pb, respectively) in geological relevant environments (e.g., Ertl, Bačík, 2020; Vereshchagin et al., 2020). A previous investigation of synthetic tourmalines confirmed that Pb occupies the *X*-site of the tourmaline crystal structure (Vereshcha-

Table 1. Chemical composition (wt %) of the tourmalines from Irkutianka and Novaya veins
Таблица 1. Химический состав (мас. %) турмалина из жил Иркутянка и Новая

Sample No	sm21-4			sm21-3				sm21-2		sm21-1		1015f*	1337f*
	1	2	3	1	2	3	4	1	2	1	2		
SiO_2	36.57	37.72	37.27	37.43	37.03	37.53	38.36	37.00	36.34	37.19	36.83	35.58 (35.25–36.09)	35.85 (35.44–36.26)
Al_2O_3	40.02	40.81	39.17	40.12	40.64	40.81	41.91	40.95	39.99	38.95	38.64	37.88 (37.41–38.33)	38.12 (37.54–38.62)
TiO_2	0.20	–	0.31	–	–	–	–	0.27	0.48	0.21	0.45	0.64 (0.62–0.66)	0.55 (0.47–0.58)
MnO_{total}	2.75	1.16	2.02	–	–	–	–	1.39	2.28	2.51	4.86	6.43 (6.26–6.53)	6.14 (6.09–6.27)
FeO_{total}	0.58	–	–	–	–	–	–	0.17	0.29	0.82	1.96	–	–
ZnO	–	–	–	–	–	–	–	–	–	–	–	0.12 (0–0.28)	–
PbO	2.09	0.10	0.29	–	0.19	–	0.20	–	–	–	–	–	–
Bi_2O_3	0.32	–	–	2.08	0.85	0.34	0.28	–	–	–	–	–	–
Na_2O	1.94	1.66	1.79	1.06	1.17	1.38	1.12	1.72	1.76	2.39	2.22	2.27 (2.20–2.33)	2.31 (2.01–2.51)
K_2O	–	–	–	–	–	–	–	–	–	–	–	0.03 (0.01–0.04)	0.03 (0.01–0.04)
CaO	0.65	1.28	1.42	2.45	2.23	1.65	2.15	0.85	1.23	0.31	0.69	1.37 (1.31–1.42)	1.43 (1.37–1.48)
Li_2O**	1.50	1.91	1.91	2.14	2.03	2.07	2.04	1.73	1.60	1.70	1.11	1.65 (1.61–1.68)	1.72 (1.66–1.79)
F	1.59	1.37	1.80	1.60	1.36	1.38	1.29	1.20	1.60	1.42	1.44	1.24 (1.22–1.27)	1.35 (1.31–1.39)
H_2O_{calc}	2.40	2.79	2.52	2.34	2.52	2.76	2.70	2.86	2.52	2.83	2.51	3.13	3.09
B_2O_{3clac}	10.74	10.94	10.78	10.81	10.79	10.89	11.12	10.86	10.71	10.76	10.77	10.75	10.82
–O=F	–0.67	–0.58	–0.76	–0.67	–0.57	–0.58	–0.54	–0.51	–0.64	–0.60	–0.61	–0.52	–0.57
Total	101.36	99.74	99.29	100.04	98.81	98.80	101.17	99.01	98.72	99.08	101.48	100.57	100.84

Table 1. (Contd.)

Sample No		sm21-4			sm21-3				sm21-2		sm21-1		1015f*	1337f*
		1	2	3	1	2	3	4	1	2	1	2		
Atomic proportion normalized to 15 ($T + Y + Z$) atoms per formula unit (*apfu*)														
X	Na	0.61	0.51	0.56	0.33	0.37	0.43	0.34	0.53	0.55	0.75	0.69	0.71	0.72
	K												0.01	0.01
	Ca	0.11	0.22	0.25	0.42	0.38	0.28	0.36	0.15	0.21	0.05	0.12	0.24	0.25
	Pb	0.09	0.00	0.01		0.01		0.01						
	Bi	0.01			0.09	0.04	0.01	0.01						
	□	0.18	0.27	0.18	0.16	0.21	0.28	0.28	0.32	0.23	0.20	0.19	0.04	0.02
Y + Z	Al	7.55	7.62	7.44	7.60	7.69	7.67	7.72	7.61	7.55	7.42	7.30	6.96	6.98
	Li	0.98	1.22	1.24	1.38	1.31	1.33	1.28	1.13	1.05	1.10	0.73	1.07	1.11
	Mn	0.38	0.16	0.27					0.20	0.31	0.34	0.66	0.88	0.84
	Fe	0.07							0.03	0.04	0.11	0.26		
	Zn												0.01	–
	Ti	0.02		0.04					0.03	0.06	0.03	0.05	0.08	0.07
	Total	9.00	9.00	9.00	8.98	9.00	9.00	9.00	9.00	9.00	9.00	9.00	9.00	9.00
T	Si	5.92	5.99	6.01	6.02	5.97	5.99	6.00	5.92	5.90	6.00	5.94	5.75	5.76
	Al	0.08	0.01			0.03	0.01		0.08	0.10		0.06	0.25	0.24
	Total	6.00	6.00	6.01	6.02	6.00	6.00	6.00	6.00	6.00	6.00	6.00	6.00	6.00
V + W	F	0.81	0.69	0.92	0.81	0.69	0.70	0.64	0.61	0.78	0.73	0.74	0.63	0.69
	O	0.59	0.35	0.37	0.68	0.59	0.36	0.54	0.33	0.49	0.22	0.56		
	OH	2.60	2.96	2.72	2.51	2.71	2.94	2.82	3.06	2.73	3.05	2.70	3.37	3.31
	Total	4.00	4.00	4.00	4.00	4.00	4.00	4.00	4.00	4.00	4.00	4.00	4.00	4.00

Samples sm21-4, sm21-3, sm21-2, sm21-2 are from the Irkutianka vein; 1015f and 1337f – from the Novaya vein. * – mean of 6 analyses, range in parentheses; – below detection limit; ** – calculated based on Pesquera (2016) for samples from the Irkutianka vein and measured by LA-ICP-MS for samples from the Novaya vein (mean of 10 analyses for each sample, range in parentheses).

gin et al., 2020), while reliable information on Bi site preference is not available. Unfortunately, the Bi content of the tourmalines under study is too low (<0.10 *apfu*) and Bi-rich zones are too small to provide SCXRD study. There are limited data on nine-coordinated Bi^{3+} in inorganic compounds (e.g., Siidra et al., 2020), while most Bi-rich minerals contain Bi in octahedron (e.g., Zubkova et al., 2002) or eight-coordinated polyhedra (e.g., Kasatkin et al., 2020). However, we can suppose that Bi occupies nine-coordinated *X*-site as its ionic radii is smaller than that of Pb^{2+} and bigger than that of Ca^{2+} (Shannon, 1976). After the discovery of Ln^{3+}-rich tourmalines (Ln^{3+} = La, Eu, Nd, Yb) with nine-coordinated lanthanides (Vereshchagin et al., 2021), one can suppose that other trivalent cations could also occupy the *X*-site. So we can predict that the general classification scheme of tourmalines based on *X*-site occupancy would include not only vacancy, univalent (e.g., Na, K) and divalent (e.g., Ca, Pb) cations, but also trivalent (e.g., Bi) cations. On the basis of the data on the influence of the chemical composition and cation oxidation state on the pyroelectric effect of tourmalines, we can predict that tourmalines, which contain trivalent cations at the *X*-site should also have enhanced pyroelectric properties (Chernyshova et al., 2021).

ACKNOWLEDGMENTS

The authors are grateful to Dr. P.B. Sokolov from Ltd SOKOLOV and K.A. Bukholcev for providing the samples from the Irkutianka vein and V.V. Muravleva, A.D. Kasatkina and M.D. Milshina for their photographing. We acknowledge very helpful comments from Dr. I.A. Baksheev, who reviewed the article. The authors thank resource centers of Saint Petersburg State University (Centre for X-ray Diffraction Studies, Microscopy and Microanalysis and Geomodel) for providing instrumental and computational resources. This work was supported by the grant of the President of the Russian Federation MK-1832.2021.1.5.

REFERENCES

Abduriyim A., Kitawaki H., Furuya M., Schwarz D. "Paraíba"-type copper-bearing tourmaline from Brazil, Nigeria, and Mozambique: Chemical fingerprinting by LA-ICP-MS. *Gems Gemol.* **2006**. Vol. 42. P. 4–21.

Badanina E.V., Gordienko V.V., Wiechovski A., Friedrich G. Sc- and *REE*-bearing ixiolite and associated minerals from the Sosedka pegmatite vein in the Malkhan pegmatite field, Central Transbaikal region. *Geol. Ore Deposits*. **2008**. Vol. 50. P. 772–781.

Baksheev I., Prokof'ev V.Y., Zaraisky G.P., Chitalin A.F., Rogacheva L.I., Gorelikova N.V., Kononov O.V. Tourmaline as a prospecting guide for the porphyry-style deposits. *Eur. J. Miner.* **2012**. Vol. 25. P. 957–979.

Bloss F.D., Gunter M., Shu C.S., Wolfe H.E. The Gladstone-Dale constants: A new approach. *Canad. Miner.* **1983**. Vol. 21. N. 1. P. 93–99.

Bosi F., Skogby H., Agrosì G., Scandale E. Tsilaisite, $NaMn_3Al_6(Si_6O_{18})(BO_3)_3(OH)_3OH$, a new mineral species of the tourmaline supergroup from Grotta d'Oggi, San Pietro in Campo, island of Elba, Italy. *Amer. Miner.* **2012**. Vol. 97. P. 989–994.

Bosi F., Andreozzi G.B., Agrosì G., Scandale E. Fluor-tsilaisite, $NaMn_3Al_6(Si_6O_{18})(BO_3)_3(OH)_3F$, a new tourmaline from San Piero in Campo (Elba, Italy) and new data on tsilaisitic tourmaline from the holotype specimen locality. *Miner. Mag.* **2015**. Vol. 79. P. 89–101.

Bosi F., Pezzotta F., Altieri A., Andreozzi G.B., Ballirano P., Tempesta G., Cempírek J., Škoda R., Filip J., Čopjakovà R., Novák M., Kampf A.R., Scribner E.D., Groat L.A., Evans R.J. Celleriite, $\square(Mn_2^{2+}Al)Al_6(Si_6O_{18})(BO_3)_3(OH)_3(OH)$, a new mineral species of the tourmaline supergroup. *Amer. Miner.* **2022a**. Vol. 107. P. 31–42.

Bosi F., Pezzotta F., Skogby H., Altieri A., Hålenius U., Tempesta G., Cempírek J. Princivalleite, $Na(Mn_2Al)Al_6(Si_6O_{18})(BO_3)_3(OH)_3O$, a new mineral species of the tourmaline supergroup from Veddasca Valley, Varese, Italy. *Miner. Mag.* **2022b**. Vol. 86. P. 78–86.

Burns P.C., MacDonald D.J., Hawthorne F.C. The crystal chemistry of manganese-bearing elbaite. *Canad. Miner.* **1994**. Vol. 32. P. 31–41.

Chernyshova I.A., Vereshchagin O.S., Malyshkina O. V, Goncharov A.G., Kasatkin I.A., Murashko M.N., Zolotarev A.A., Frank-Kamenetskaya O.V. Tourmalines pyroelectric effect depending on the chemical composition and cation oxidation state. *J. Solid State Chem.* **2021**. Vol. 303. P. 122512.

Ertl A., Bačík P. Considerations about bi and pb in the crystal structure of Cu-bearing tourmaline. *Minerals*. **2020**. Vol. 10. P. 1–15.

Ertl A., Hughes J.M., Prowatke S., Rossman G.R., London D., Fritz E.A. Mn-rich tourmaline from Austria: structure, chemistry, optical spectra, and relations to synthetic solid solutions. *Amer. Miner.* **2003**. Vol. 88. P. 1369–1376

Ertl A., Hughes J.M., Prowatke S., Ludwig T., Brandstätter F., Körner W., Dyar M.D. Tetrahedrally coordinated boron in Li-bearing olenite from "mushroom" tourmaline from Momeik, Myanmar. *Canad. Miner.* **2007**. Vol. 45. P. 891–899.

Ertl A., Kolitsch U., Dyar M.D., Hughes J.M., Rossman G.R., Pieczka A., Henry D.J., Pezzotta F., Prowatke S., Lengauer C.L., Korner W., Brandstatter F., Francis C.A., Prem M., Tillmanns E. Limitations of Fe^{2+} and Mn^{2+} site occupancy in tourmaline: Evidence from Fe2+- and Mn2+-rich tourmaline. *Amer. Miner.* **2012**. Vol. 97. P. 1402–1416.

Ertl A., Topa D., Giester G., Rossman G.R., Tillmanns E., Konzett J. Sr-bearing high-pressure tourmaline from the Kreuzeck Mountains, Eastern Alps, Austria. *Eur. J. Miner.* **2019**. Vol. 31. P. 791–798.

Fritsch E., Shigley J.E., Rossman G.R., Mercer M.E., Muhlmeister S.M., Moon M. Gem-quality cuprian-elbaite tourmalines from São José da Batalha, Paraíba, Brazil. *Gems Gemol.* **1990**. Vol. 26. P. 186–205.

Henn U., Bank H., Bank F.H. Transparent bright blue Cu-bearing tourmalines from Paraiba, Brazil. *Miner. Mag.* **1990**. Vol. 54. P. 553–557.

Henry D.J., Novák M., Hawthorne F.C., Ertl A., Dutrow B.L., Uher P., Pezzotta F. Nomenclature of the tourmaline-supergroup minerals. *Amer. Miner.* **2011**. Vol. 96. P. 895–913.

Johnson M.L., Wentzell C.Y., Elen S. Multicolored bismuth-bearing tourmaline from Lundazi, Zambia. *Gems Gemol.* **1997**. Vol. 33. P. 204–211.

Kasatkin A.V., Britvin S.N., Peretyazhko I.S., Chukanov N.V., Škoda R., Agakhanov A.A. Oxybismutomicrolite, a new pyrochlore-supergroup mineral from the Malkhan pegmatite field, Central Transbaikalia, Russia. *Miner. Mag.* **2020**. Vol. 84. P. 444–454.

Kubernátová M., Cempírek J. Crystal chemistry of Pb-rich tourmaline from pegmatite in Minh Tien, Vietnam. In: *9th European Conference on Mineralogy and Spectroscopy*, ECMS 2019, **2019**.

Kutzschbach M., Wunder B., Krstulovic M., Ertl A., Trumbull R., Rocholl A., Giester G. First high - pressure synthesis of rossmanitic tourmaline and evidence for the incorporation of Li at the *X* site. *Phys Chem Miner.* **2017**. Vol. 44 P. 353–363.

Lebedev A. On lead-bearing tourmaline from the Maly Khingan, *Comptes Rend Acad. Sci. U.R.S.S.* **1937**. Vol. 3. P. 127–128 (*in Russian*).

Li Y., Huang Z., Liu Y., Fang M. Characterization of dielectric performance of tourmaline single crystals from Yunnan, China. *Cryst. Eng. Comm.* **2012**. Vol. 14. P. 7153–7156.

London D., Ertl A., Hughes J.M., Morgan VI G.B., Fritz E.A., Harms B.S. Synthetic Ag-rich tourmaline: Structure and chemistry. *Amer. Miner.* **2006**. Vol. 91. P. 680–684.

Lussier A., Hawthorne F. Oscillatory zoned liddicoatite from Anjanabonoina, Central Madagascar. II. Compositional variation and mechanisms of substitution. *Canad. Miner.* **2011**. Vol. 49. P. 89–104.

Merlet C. An Accurate computer correction program for quantitative electron probe microanalysis. *Microchim. Acta*. **1994**. Vol. 114/115. P. 363–376.

Peretyazhko I.S., Zagorskiy V.Y., Bobrov Y.D., First find of bismuth- and lead-rich tourmaline. *Trans.* (*Doklady*) *USSR Acad. Sci. Earth Sci. Sect.* **1989**. Vol. 307. P. 175–179 (*in Russian*).

Peretyazhko I.S., Zagorsky V.Ye., Sapozhnikov A.N., Bobrov Y.D., Rakcheev A.D. Bismutocolumbite $Bi(Nb,Ta)O_4$ – a new mineral from miarolitic pegmatites. *Zapiski RMO* (*Proc. Russian Miner. Soc.*). **1992**. Vol. 121. P. 130–134 (*in Russian*).

Pesquera A., Gil-Crespo P.P., Torres-Ruiz F., Torres-Ruiz J., Roda-Robles E. A multiple regression method for estimating Li in tourmaline from electron microprobe analyses. *Miner. Mag.* **2016**. Vol. 80. P. 1129–1133.

Pezzotta F., Laurs B.M. Tourmaline: The kaleidoscopic gemstone. *Elements.* **2011**. Vol. 7. P. 333–338.

Rossman G.R., Mattson S.M. Yellow, Mn-rich elbaite with Mn–Ti intervalence charge transfer. *Amer. Miner.* **1986**. Vol. 71. P. 599–602.

Rossman G.R., Fritsch E., Shigley J.E. Origin of color in cuprian elbaite from São José da Batalha, Paraíba, Brazil. *Amer. Miner.* **1991**. Vol. 76. P. 1479–1484.

Shannon R.D. Revised effective ionic radii and systematic studies of interatomic distances in halides and chalcogenides. *Acta Crystallogr. Sect. A 32.* **1976**. P. 751–767.

Siidra O., Charkin D., Plokhikh I., Nazarchuk E., Holzheid A., Akimov G. Expanding family of litharge-derived sulfate minerals and synthetic compounds: Preparation and crystal structures of $[Bi_2CuO_3]SO_4$ and $[Ln_2O_2]SO_4$ (*Ln* = Dy and Ho). *Minerals*. **2020**. Vol. 10. P. 1–10.

Simmons W.B., Falster A.U., Laurs B.M. A survey of mn-rich yellow tourmaline from worldwide localities and implications for the petrogenesis of granitic pegmatites. *Canad. Miner.* **2011**. Vol. 49. P. 301–319.

Sokolov M., Martin R. A Pb-Dominant member of the Tourmaline Group, Minh Tien Granitic Pegmatite, Luc Yen district, Vietnam. *Estud. Geológicos*. **2009**. Vol. 19. P. 352–353.

Staatz M.H., Murata K.J., Glass J.J. Variation of composition and physical properties of tourmaline with its position in the pegmatite. *Amer. Miner.* **1955**. Vol. 40. P. 789–804.

Sunde Ø., Friis H., Andersen T., Trumbull R.B., Wiedenbeck M., Lyckberg P., Agostini S., Casey W.H., Yu P. Boron isotope composition of coexisting tourmaline and hambergite in alkaline and granitic pegmatites. *Lithos*. **2020**. Vol. 352–353. P. 105293.

Swadźba-Kwaśny M. Lead: Inorganic Chemistry. *Encycl. Inorg. Bioinorg. Chem*. **2015**. P. 1–24.

Van Hinsberg V.J., Henry D.J., Marschall H.R. Tourmaline: An ideal indicator of its host environment. *Canad. Miner.* **2011**. Vol. 49. P. 1–16.

Vereshchagin O.S., Wunder B., Britvin S.N., Frank-Kamenetskaya O.V., Wilke F.D.H., Vlasenko N.S., Shilovskikh V.V. Synthesis and crystal structure of Pb-dominant tourmaline. *Amer. Miner.* **2020**. Vol. 105. P. 1589–1592.

Vereshchagin O.S., Britvin S.N., Wunder B., Frank-Kamenetskaya O.V., Wilke F.D.H., Vlasenko N.S., Shilovskikh V.V, Bocharov V.N., Danilov D.V. Ln^{3+} (Ln^{3+} = La, Nd, Eu, Yb) incorporation in synthetic tourmaline analogues: Towards tourmaline REE pattern explanation. *Chem. Geol.* **2021**. Vol. 584. P. 120526.

Whitmire K.H. Bismuth: Inorganic Chemistry, Encyclopedia of Inorganic and Bioinorganic Chemistry, **2014**.

Wunder B., Berryman E., Plessen B., Rhede D., Koch-Müller M., Heinrich W. Synthetic and natural ammonium-bearing tourmaline. *Amer. Miner.* **2015**. Vol. 100. P. 250–256.

Xia M., Kang L. Tourmaline with ultraviolet optical nonlinearity: Emergent material discovery from mineral. *J. Alloys Compd*. **2022**. Vol. 892. P. 162235.

Zagorsky V.Ye. Malkhan gem tourmaline deposit: types and nature of miaroles. *Doklady Earth Sci*. **2010**. Vol. 431. P. 314–317.

Zagorsky V.Ye. Sosedka pegmatite body at the Malkhan gem tourmaline deposit, Transbaikalia: composition, inner structure, and petrogenesis. *Petrology*. **2015**. Vol. 23. P. 68–92.

Zagorsky V.Ye., Peretyazhko I.S. Pegmatites with precious stones of the Central Transbaikalia. Novosibirsk: Nauka Press, **1992**. 224 p. (*in Russian*).

Zagorsky V.Ye., Peretyazhko I.S., Shmakin B.M. Miarolitic Pegmatites. In: *Granitic Pegmatites*, Vol. 3. Novosibirsk: Nauka, **1999**. 488 p. (*in Russian*).

Zubkova N.V., Pushcharovsky D.Y., Giester G., Smolin A.S., Tillmanns E., Brandstätter F., Hammer V., Peretyazhko I.S., Sapozhnikov A.N., Kashaev A.A. Bismutocolumbite, $Bi(Nb_{0.79}Ta_{0.21})O_4$, stibiocolumbite, $Sb(Nb_{0.67}Ta_{0.33})O_4$, and their structural relation to the other ABO_4 minerals with stibiotantalite ($SbTaO_4$) structure. *Neues Jahrb. fur Mineral. Monatshefte.* **2002**. Vol. 2002. P. 145–159.

НОВЫЕ ДАННЫЕ О Bi-, Pb-СОДЕРЖАЩЕМ И ОБОГАЩЕННОМ Mn ТУРМАЛИНЕ ИЗ МАЛХАНСКОГО ПЕГМАТИТОГО ПОЛЯ (ЗАБАЙКАЛЬЕ)

Д. чл. О. С. Верещагин[1], *, А. В. Касаткин[2], Р. Шкода[3]

[1]Кафедра минералогии, Институт наук о Земле, Санкт-Петербургский государственный университет, Университетская наб., 7/9, Санкт-Петербург, 199034 Россия

[2]Минералогический музей им. А.Е. Ферсмана РАН, Ленинский пр., 18-2, Москва, 119071 Россия

[3]Кафедра геологических наук, Масариков университет, Брно, Чехия

**e-mail: o.vereshchagin@spbu.ru*

Свинец- и/или висмут-содержащий турмалин редок в природе, в то время как марганец является типичным примесным элементом в этом минерале. В настоящей работе представлены новые данные о турмалине Малханского пегматитого поля: (1) Bi- (до ~2 мас. % Bi_2O_3), Pb- (до ~2 мас. % PbO) и Mn-содержащих (до ~5 мас. % MnO) кристаллах турмалина из жилы Иркутянка и (2) богатых марганцем (до ~6.5 мас. % MnO) кристаллах турмалина из жилы Новая. Четыре кристалла турмалина ювелирного качества из жилы Иркутянка (sm21-1, sm21-2, sm21-3, and sm21-4) различной окраски (желтые, бесцветные и красные) и морфологии (вытянутые и уплощенные) были изучены методами оптической и электронной микроскопии и энергодисперсионной рентгеновской спектроскопии. Два удлиненных кристалла турмалина желтого цвета из жилы Новая (1015f и 1377f) были дополнительно исследованы методами WDS и LA-ICP-MS. Все изученные образцы турмалина из жилы Иркутянка принадлежат к ряду фтор-эльбаит – фтор-лиддикоатит и имеют хорошо выраженную зональность (Na/Ca и Li/Mn/Fe). Турмалин из жилы Новая незональный и принадлежат к обогащенной марганцем (Mn до 0.88 к.ф.) разновидности фтор-эльбаита. Наличие (или отсутствие) окраски турмалина напрямую связано с содержанием катионов переходных металлов. Бесцветный турмалин sm21-4 содержит постоянную примесь висмута, содержание которого уменьшается от края кристалла к центру (от 0.09 до 0.01 к.ф.). Содержание висмута в этом турмалине близко к предельно высокому из ранее известных в природе. Свинец обнаружен в бесцветном образце sm21-4 и розово-прозрачном кристалле sm21-3. Только внутренняя часть турмалина sm21-3 содержит свинец (<0.2 мас. % PbO), в то время как наиболее обогащенные свинцом зоны (размером до 30 мкм; Pb до 0.09 к.ф.) были обнаружены во внешней части кристалла sm21-4. Высказано предположение, что Pb^{2+} и Bi^{3+} заселяют девяти-координированный XO_9-полиэдр в кристаллической структуре турмалина.

Ключевые слова: турмалин, свинец, висмут, марганец, Малханское пегматитовое поле